Eur. Phys. J. D **6**, 221–233 (1999)

THE EUROPEAN PHYSICAL JOURNAL D

EDP Sciences

Simulating the thermal stability and phase changes of small carbon clusters and fullerenes

P.A. Marcos[a], J.A. Alonso, A. Rubio, and M.J. López[b]

Departamento de Física Teórica, Universidad de Valladolid, 47011 Valladolid, Spain

Received: 25 March 1998 / Received in final form: 30 October 1998

Abstract. The thermal stability, phases and phase changes of small carbon clusters and fullerenes are investigated by constant energy Molecular Dynamics simulations performed over a wide range of temperatures, *i.e.*, from $T = 0$ K to above the melting point of graphitic carbon. The covalent bonds between the carbon atoms in the clusters are represented by the many-body Tersoff potential. The zero temperature structural characteristics of the clusters, *i.e.*, the minimum energy structures as well as the isomer hierarchy can be rationalized in terms of the interplay between the strain energy (due to the surface curvature) and the number of dangling bonds in the cluster. Minimization of the strain energy opposes the formation of cage structures whereas minimization of the number of dangling bonds favors it. To obtain a reliable picture of the processes experienced by carbon clusters as a function of temperature, both thermal and dynamical characteristics of the clusters are carefully analyzed. We find that higher excitation temperatures are required for producing structural transformations in the minimum energy structures than in higher lying isomers. We have also been able to unambiguously identify some structural changes of the clusters occurring at temperatures well below the melting-like transition. On the other hand, the melting-like transition is interrupted before completion, *i.e.*, the thermal decomposition of the clusters (evaporation or ejection of C_2 or C_3 units) occurs, from highly excited configurations, before the clusters have fully developed a liquid-like phase. Comparison with experiments on the thermal decomposition of C_{60} and a discussion of the possible implications of our results on the growth mechanisms leading to the formation of different carbon structures are included.

PACS. 36.40.Ei Phase transitions in clusters – 61.48.+c Fullerenes and fullerene-related materials – 82.30.Qt Isomerization and rearrangement

1 Introduction

Looking at the mass spectrum of carbon clusters published in 1984 by Rohlfing and coworkers [1], one clearly recognizes the prominent peak corresponding to C_{60}. This peak in the mass spectrum was not so impressive, though, as to make anyone guess at that time the uniqueness of this hollow-cage all-carbon molecule, the buckminsterfullerene [2] (buckyball for short). Under the right experimental conditions [3] one can produce macroscopic quantities of C_{60} and the buckyball is, essentially, the only C_{60} isomer (among the 1812 possible fullerene isomers of C_{60} [4]) present in those macroscopic samples. Puzzling enough, stability arguments in their own would not predict nor even justify the preferential formation of the buckyball under certain conditions. One has to bear in mind that this is not the most stable form of carbon, larger fullerenes as well as graphite have higher binding energies per atom than the buckyball. Moreover, the small energy difference between the buckyball and other fullerene isomers of C_{60} (of the order of the energy difference between graphite and diamond) does not rule out in itself the formation of those isomers in macroscopic quantities. What makes, then, nature so easily find the way to producing this highly symmetric molecule?

Even after this, carbon had still a lot of excitement awaiting us behind the door. Only a few years after the discovery of fullerenes new carbon structures were observed such as nanotubes [5], onions [6], and, more recently, cones [7]. All these structures have in common being formed by networks of sp^2-bonded carbon which roll themselves up into ball, tube, or cone structures so as to minimize the number of dangling bonds. Besides the basic interest in these network-like carbon structures there are also well founded expectations of possible practical applications of some of these novel carbon-based materials. However, the practical use of any of these materials would require its production under well controlled conditions. It is, then, of fundamental concern understanding the growth mechanisms leading to the

[a] *Present address*: Departamento de Física, Universidad de Burgos, Burgos, Spain

[b] e-mail: maria@fixat8.fam.cie.uva.es

formation of each of these new carbon structures. As has been recognized by several authors, fullerenes, tubes, and other related carbon structures are produced under highly nonequilibrium conditions which makes determining the growth mechanisms of these nanostructures extremely difficult.

In this paper we concentrate on the problem of small carbon clusters and fullerenes. Several growth models of C_{60} have been proposed in the literature, *e.g.* the pentagon road model, the fullerene road model, or the cycloaddition model [8]. However, none of these models fits all the experimental evidence well. Other important drawbacks of these models are that they neither explain the absence of other cluster sizes, nor lead to a preferential formation of the buckyball with respect to other fullerene isomers of C_{60}. In addition, all these models require, in the last stages of formation of the buckyball, an annealing mechanism, involving the rearrangement of pentagons and hexagons, driving the fullerene isomers of C_{60} into the most stable structure, the buckyball, which is the only 60-atom fullerene having I_h symmetry and no adjacent pentagons. Even this last process of annealing the fullerene structures down to the buckyball is not well understood. As we have mentioned above, the difficulty in understanding the formation mechanism of fullerenes stems from the fact that their production does not take place under thermal equilibrium conditions but rather it involves a kinetics-controlled process. As a consequence, knowing the zero temperature properties of small carbon clusters and fullerenes is not sufficient for explaining their production. For instance a genetic algorithm [9] has been applied successfully for obtaining the minimum energy structures of several carbon clusters, including C_{60}. However, this algorithm does not provide any insight into the growth process. Dynamical simulations on the nucleation of C_{60} give qualitative insights to the formation of carbon fullerenes [10]. Nucleation of C_{60} has been simulated both by annealing a hot carbon plasma (formed exactly by 60 carbon atoms in a box) and by monomer addition to a small carbon seed. These simulations show that clustering occurs readily (under the right annealing or growth rate conditions, respectively) producing cage structures for C_{60}, although not the ground state. Simulations have also been performed for a few carbon atoms in a box [11]. Under suitable temperature control the simulation produced several cage structures. One of the cages was a C_{60} cluster with some dangling bonds, heptagons and neighboring pentagons. When removed from the box and annealed this cluster achieved the perfect I_h symmetry but if the cluster is left in the original simulation box its growth continues. The thermal stability and decomposition kinetics of C_{60} molecules (both in the gas phase [12] and in the solid state [13,14]) have been studied in order to provide further understanding on the chemistry of fullerene formation. Learning about the thermal behaviour (including the possible phases, isomerization transitions and phase changes) of small carbon clusters and fullerenes [15–19] would help to understand the processes and mechanisms leading to the formation of buckyballs, fullerene-like structures, and other carbon polytypes. This is the primary goal of this paper. As the first step we have investigated the zero temperature behaviour, *i.e.*, the possible isomeric forms, of small carbon clusters and the C_{60} fullerene using the thermal quenching procedure. The minimum energy structures as a function of cluster size and the isomer hierarchy for a given cluster size can be understood in terms of two single concepts: "curvature" and "dangling bonds". Subsequently, we have performed extensive Molecular Dynamics simulations to investigate the finite-temperature behaviour of the clusters. We consider cluster temperatures ranging from $T = 0$ K up to above the melting point of graphitic carbon, not only for the minimum energy structures but also for several relevant isomers. Thermal characteristics of the clusters such as the caloric curve (kinetic temperature *vs.* total energy), the root mean square bond length fluctuation, and the specific heat are analyzed. These magnitudes have proved to be quite informative about phases and phase changes in dynamical studies of Lennard-Jones and metal clusters. However, do not reflect some of the low-temperature structural transformations (isomerization transitions) occurring in carbon clusters. Therefore to obtain a more detailed and accurate picture of the processes experienced by carbon clusters as a function of temperature, we combine the previous thermal analysis with a dynamical analysis of the trajectories. The short-time-averaged kinetic energy is a magnitude more sensitive to the cluster structure. Its time evolution, then, together with a thermal quenching analysis of the simulation trajectories, provides information on the time evolution of the structural changes of the clusters, even at low temperatures. We find that the minimum energy structures are more resistant (*i.e.*, higher excitation energies are needed) to structural changes than higher lying isomers. On the other hand, some structural transformations of the clusters are observed at temperatures well below the melting-like transition. Another salient finding of our investigations is that carbon clusters start to evaporate atoms or C_2 or C_3 units before fully developing a liquid-like phase. However, the thermal decomposition of the clusters occurs from highly excited configurations, in agreement with the experimental findings [12,13]. These and some related thermal features of carbon clusters will be, for certain, of relevance for understanding and explaining the growth mechanisms of different carbon structures.

The structure of the paper is as follows. In Section 2 we present the many-body interatomic potential, Tersoff potential, used to describe the interactions between the carbon atoms in the clusters and some details about the dynamical simulations performed here. Section 3 presents the results of the simulations: firstly, the isomer hierarchy of small carbon clusters and C_{60} and secondly their thermal behaviour. A discussion of the results is also included. We finish with some conclusions in Section 4.

2 Theoretical background

In this paper we have performed extensive constant energy Molecular Dynamics (MD) simulations of small carbon clusters and fullerenes. From the simulations we extract

the structural, dynamical and thermal characteristics of these systems. The time evolution of the system is obtained by integrating numerically (using the velocity version of the Verlet algorithm [20]) the classical Newtonian equations of motion. A time step of 0.2 fs yields conservation of the total energy within 0.01% for trajectories lasting 2.5×10^5 time steps.

Performing MD simulations requires knowledge of the interatomic interactions between the atoms in the system under consideration (small carbon clusters and fullerenes in this case). The interatomic interactions could be obtained, in principle, from *ab initio* (first principles) calculations. However, this is a very demanding (time consuming) task even for not too large systems when one is concerned with thermal and dynamical properties of the system. As an alternative one can use a computationally efficient empirical potential to mimic the interatomic interactions between the atoms in the system. Clearly, the accuracy and reliability of the chosen potential for describing the physical system of interest should be carefully checked.

Throughout this paper we use Tersoff's potential [21] to mimic the covalent bond between the carbon atoms in small clusters and fullerenes. This potential goes beyond the three-body potentials considered in the literature for describing covalent systems. The Tersoff potential incorporates "effective" many-body interactions following the bond order ideas introduced by Abell [22]. The bond order (*i.e.*, the strength of a bond) depends on the local environment. The leading term of the bond order can be expressed as a function of coordination. Moreover, an explicit dependence on the bond angles is incorporated in Tersoff's potential in order to favor bond angles corresponding to the sp^2 and sp^3 hybridizations of carbon. The interatomic potential is written "formally" as a sum of pairwise interactions

$$V = \frac{1}{2} \sum_{i,j(\neq i)=1}^{N} f_{\mathrm{c}}(r_{ij}) \left[f_{\mathrm{R}}(r_{ij}) + b_{ij} f_{\mathrm{A}}(r_{ij}) \right] , \qquad (1)$$

where N is the number of atoms in the cluster and f_{R} and f_{A} represent repulsive and attractive pair potentials, respectively,

$$\begin{aligned} f_{\mathrm{R}}(r_{ij}) &= A e^{(-\lambda_1 r_{ij})} , \\ f_{\mathrm{A}}(r_{ij}) &= -B e^{(-\lambda_2 r_{ij})} . \end{aligned} \qquad (2)$$

The bond order coefficient b_{ij} carries the many-body character of the potential and is written as

$$\begin{aligned} b_{ij} &= \left(1 + \beta^n \xi_{ij}^n\right)^{-\frac{1}{2n}} , \\ \xi_{ij} &= \sum_{k(\neq i,j)=1}^{N} f_{\mathrm{c}}(r_{ik}) g(\theta_{ijk}) , \\ g(\theta_{ijk}) &= 1 + \frac{c^2}{d^2} - \frac{c^2}{d^2 + (h - \cos\theta_{ijk})^2} , \end{aligned} \qquad (3)$$

where θ_{ijk} is the bond angle between the ij and the ik bonds. A smooth cut-off function f_{c} is used to limit the range of the potential. In practice this function is chosen to cut the interactions between the first and the second neighboring shells. In this work we use a Fermi-type cut-off function [19]

$$f_{\mathrm{c}}(r_{ij}) = \frac{1}{1 + e^{\frac{r_{ij} - r_0}{D}}} , \qquad (4)$$

with values of the parameters $r_0 = 2.05$ Å and $D = 6.13 \times 10^{-2}$ Å. The use of this function instead of the original cut-off function proposed by Tersoff improves the energy conservation in the dynamical simulations. The reason being that the Fermi function is derivable with continuity to all orders whereas the cut-off function used by Tersoff is derivable with continuity only up to first order.

The values of the parameters of the potential for carbon: $A = 1393.6$ eV, $B = 346.74$ eV, $\lambda_1 = 3.4879$ Å^{-1}, $\lambda_2 = 2.2119$ Å^{-1}, $\beta = 1.5724 \times 10^{-7}$, $n = 0.72751$, $c = 38049$, $d = 4.3484$, and $h = -0.57058$, have been obtained by fitting the potential to the cohesive energies of several real and hypothetical carbon polytypes (*i.e.*, the C_2 dimer, graphite, diamond, and the simple cubic, the body centered cubic, and the face centered cubic lattices) as well as to the lattice constant and bulk modulus of diamond. In addition a value of the vacancy formation energy in diamond of at least 4 eV was required. This potential reproduces adequately the structural features and the energetics of carbon over a wide range of configurations (*i.e.*, coordinations), the elastic moduli and phonon frequencies of diamond, the in-plane elastic constants of graphite and the energies of point defects both in diamond and graphite. This makes this potential reliable also for cluster studies. However, for the correct interpretation of the predictions and results obtained using Tersoff's potential, one should also be aware of its limitations. On the one hand, linear chains and ring structures, characterized by large bond angles, are not well described by the Tersoff potential. The reason being that this potential favors the formation of bond angles close to $\frac{2}{3}\pi$, characteristic of the sp^2 and sp^3 hybridizations of carbon. Consequently, the results for structures with exposed edges are only qualitative. On the other hand, the melting temperature of carbon comes out about 40% higher than the experimental one [23]. Therefore, when comparing to experiments, the temperatures presented in this paper should be rescaled by the corresponding factor.

3 Results and discussion

3.1 Isomer hierarchy

Finite systems at finite temperatures may exhibit many different geometrical configurations (isomeric forms). For this reason it is useful to study the possible isomeric forms of a system before trying to understand its finite-temperature behaviour. However, as is well known since

the early days of cluster studies, the number of possible isomers is huge even for small/medium size clusters (*e.g.*, the number of isomers of a 55-atom cluster has been estimated [24] to be 8.3×10^{11}). This makes completely out of scope the calculation of even a fraction of the isomers of clusters in the size range of a few tens of atoms or larger. Still one could try to generate a set of isomers, including eventually the minimum energy structure, sufficiently large for extracting the main structural features of the clusters and relating them to their thermal behaviour and, possibly, to their growth mechanisms.

The study of the possible isomeric forms of carbon clusters remains still an open question [25]. On the one hand, only a relatively small number of isomers of small carbon clusters has been studied using first principles calculations. On the other hand, the theoretical predictions on the relative ordering of the isomers depend strongly on the level of the theory being used for describing the clusters. In a recent paper Jones and Seifert [26] have studied a selection of isomers of C_N clusters ($14 \leq N \leq 24$, N even) within the density functional formalism using both the local spin density approximation (LSD) and gradient corrections (GC) to the exchange-correlation energy. For every fixed type of isomer (*i.e.*, monocyclic rings, cage structures, or graphitic geometries, etc.) both models produce similar variations in the binding energy as a function of cluster size. However, the gradient corrections affect differently two different types of isomers. This results in a change in the energy ordering of the isomers with respect to the LSD calculations. For instance the minimum energy structure of C_{20} and C_{22} changes from being a cage in the LSD approximation to a monocyclic ring when one uses gradient corrections. Hartree-Fock calculations also predict the monocyclic ring as the minimum energy structure of C_{20}. However, electronic structure calculations at the level of MP2 (second-order Moller-Plesset perturbation) as well as CCSD(T) calculations [27] (coupled-cluster calculations with all single and double excitations and a perturbational estimate of some triple excitations) give the same minimum energy structure of C_{20} as LSD, a hollow cage, which is the smallest topologically possible fullerene. Still, higher level exchange-correlation functionals [25] such as B3LYP (Becke three-parameter exchange with Lee-Yang-Parr correlation) or BPW91 (Becke 1988 exchange with Perdew-Wang 1991 correlation), as well as quantum Monte Carlo approaches [28] predict the bowl structure (a portion of the C_{60} fullerene formed by a pentagonal face surrounded by five hexagons), as the most stable isomer of C_{20}. The use of semiempirical potentials for studying the isomer hierarchy of small carbon clusters is not of help for clarifying this controversy. However, the use of semiempirical potentials allows one to perform an extensive search of isomers on the potential energy surface and therefore to extract the underlying rules which determine the cluster structures.

The search of isomers has been performed using the "thermal quenching" procedure. This procedure consists in cooling down high-energy configurations, selected from high-energy trajectories, into rigid structures corresponding to local minima of the potential energy surface. To obtain a "relevant" set of isomers of small carbon clusters (one has to bear in mind that the number of isomers for clusters having a few tens of atoms is huge and, consequently, even with the help of semi-empirical potentials, it is not possible to obtain even a fraction of them) we have generated high-energy trajectories originating on different wells of the potential energy surface corresponding to different structural types known (or expected) to be relevant for carbon clusters, namely, ring, planar, bowl-type, hollow cage, and diamond structures. The initial configurations for the quenching procedure have been selected along those trajectories at time intervals corresponding to a few vibrational periods of the cluster (in practice we have selected one out of 500 configurations along a trajectory) to give the possibility for configurational changes of the cluster to occur between successive quenches. As a result, we have produced a set of about 50 to 100 different isomers for each cluster size. Since several "relevant" regions of the configuration space have been explored, we believe these sets of isomers to provide at least a qualitative picture about the structural properties of carbon clusters.

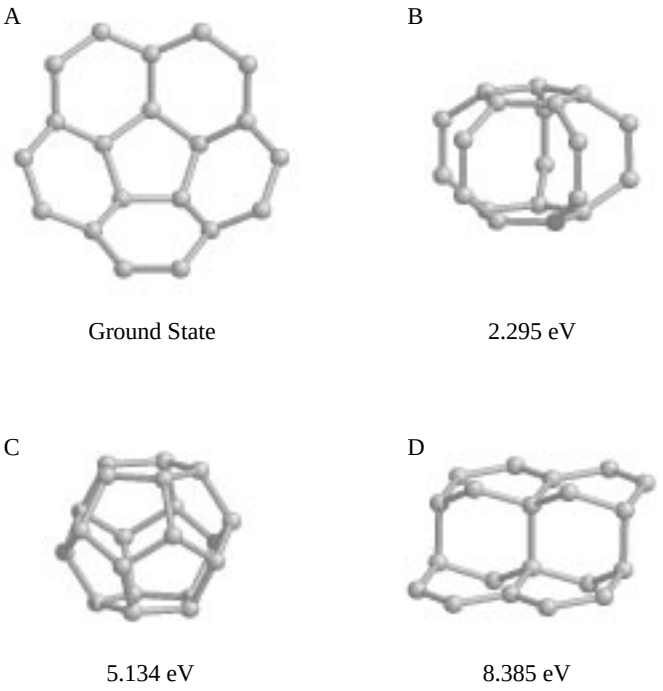

Fig. 1. Geometry of some selected isomers of C_{20}. The energies of the isomers (in eV) are measured from the minimum energy structure (bowl) of C_{20}. A: bowl structure, B: cage structure with D_{5h} symmetry, C: fullerene structure, and D: diamond-like structure.

In a previous paper [19] we have presented some of the isomeric forms of C_{13}, C_{20} and C_{32} as predicted by the Tersoff potential. Figures 1 and 2 show a selection of isomers of C_{20} and C_{60}, respectively. To understand and interpret the rules which determine the minimum energy structures of small clusters as a function of cluster size as

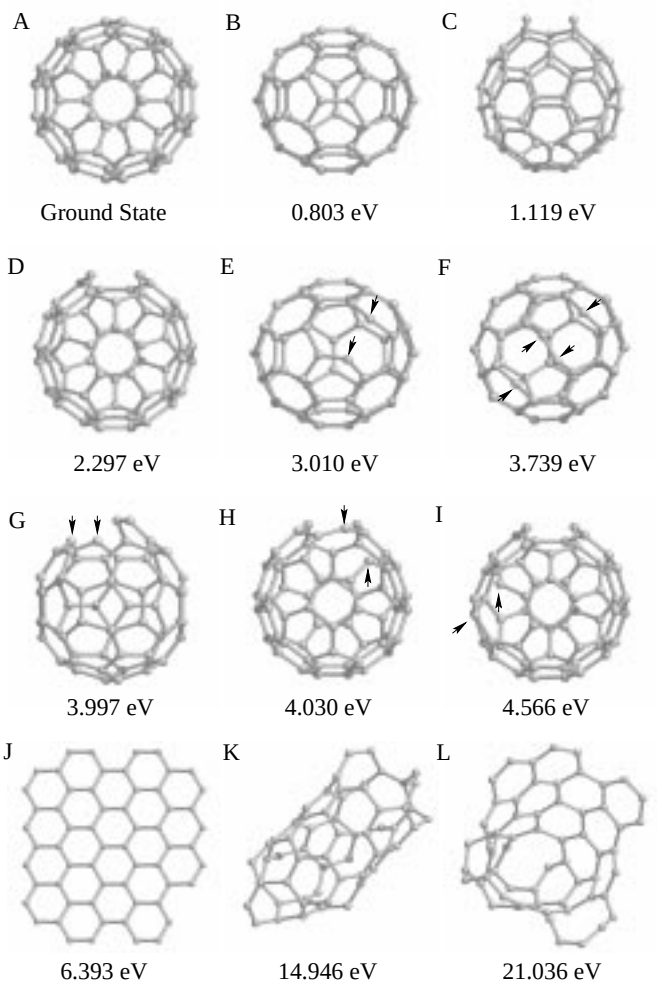

Fig. 2. Geometry of some selected isomers of C_{60}. The energies of the isomers (in eV) are measured from the minimum energy structure of C_{60}. A: buckyball, B: isomer obtained from A by performing a Stone-Wales transformation, C: isomer B with one open window between two pentagons, D: isomer A with one open window between a pentagon and a hexagon, E: isomer B with one open window between a pentagon and a hexagon, F to I: fullerene-based isomers with several open windows, J: piece of a graphene sheet, K: tubular-like structure, and L: deformed bowl-like structure. The arrows indicate some open windows in the fullerene-like isomers.

well as the isomer hierarchy for a fixed size, it is convenient to partition the energy in several contributions

$$V = \sum_{i=1}^{N} V_i^{\mathrm{ref}} + E^{\mathrm{strain}}\,, \tag{5}$$

where V_i^{ref} is the energy of an atom in an appropriately defined reference system and the strain energy, E^{strain}, represents the energy change in the cluster with respect to the reference system. For systems interacting through pairwise potentials one can consider the diatomic molecule as the reference system which allows the introduction of a rigorous definition of strain energy [29]. The choice of the reference system for many-body potentials, however, is not so inmediate since the strength of a bond depends on the local environment. In the case of carbon structures based on sp^2 networks of carbon it seems reasonable to choose the perfect graphene sheet as the reference system for 3-fold coordinated atoms and the edge atoms of a semi-infinite graphene sheet for 2-fold coordinated atoms (*i.e.*, atoms with a dangling bond)

$$V_i^{\mathrm{ref}} = \begin{cases} V_i^{\mathrm{graph}}, & \text{if } i \text{ 3-fold coordinated}\,, \\ V_i^{\mathrm{edge\text{-}graph}}, & \text{if } i \text{ 2-fold coordinated}\,, \end{cases} \tag{6}$$

where V_i^{graph} is the energy of an atom in a perfect graphene sheet and $V_i^{\mathrm{edge\text{-}graph}}$ is the energy on an edge atom in a semi-infinite graphene sheet. The cluster energy can be written as

$$V = \sum_{i=1}^{N} V_i^{\mathrm{graph}} + N_{\mathrm{d}} E^{\mathrm{dangling}} + E^{\mathrm{strain}}\,, \tag{7}$$

where N_{d} is the number of dangling bonds in the cluster and the dangling energy E^{dangling}, given by

$$E^{\mathrm{dangling}} = V_i^{\mathrm{edge\text{-}graph}} - V_i^{\mathrm{graph}}\,, \tag{8}$$

represents the loss of stability of the cluster (with respect to a perfect graphene sheet) due to the presence of dangling bonds. Equation (7) constitutes a rigorous definition of the strain energy for carbon networks. This energy represents the destabilization of the cluster, with respect to the reference system(s) due, not only to the change in the bond lengths, as is the case for pairwise potentials [29], but also to the surface curvature. Table 1 presents the total, dangling, and strain energies of the isomers of C_{20} and C_{60} shown in Figures 1 and 2, respectively.

We find that the minimum energy structure of C_{20} is the bowl isomer (structure A of Fig. 1), in agreement with the most sophisticated *ab initio* calculations [25,28]. However, one should not overemphasize this agreement for the reasons mentioned above. The bowl structure has ten dangling bonds but the strain energy associated with the cluster curvature is small (see Table 1). The lowest-energy isomers of C_{20} (not shown here) are graphene sheets and bowl-type structures, either perfect or incorporating some defects such as pentagonal or heptagonal rings. Also low-lying bowl-type isomers are produced by a window-opening mechanism in which a carbon-carbon bond breaks giving rise to an 8- or 9-membered ring. The fullerene isomer (structure C of Fig. 1), although it has no dangling bonds, comes out 5.13 eV higher in energy than the bowl minimum energy structure due to the high strain energy associated with the surface curvature (Tab. 1). Several cage isomers, lower in energy than the fullerene, are produced by opening one or several windows in the fullerene cage which releases partially the strain energy associated with the presence of adjacent pentagons in the structure. The lowest-energy cage isomer (which is 2.29 eV above the minimum energy structure) has D_{5h}

Table 1. Total energy with respect to the graphene sheet (third column), number of dangling bonds, $N_{\rm d}$, dangling energy, $N_{\rm d}E^{\rm dangling}$, and strain energy, $E^{\rm strain}$ of the isomers of C_{20} and C_{60} shown in Figures 1 and 2, respectively. All the energies are given in eV.

Cluster	Isomer	$V - \sum_i V_i^{\rm graph}$	$N_{\rm d}$	$N_{\rm d}E^{\rm dangling}$	$E^{\rm strain}$
C_{20}	A	27.794	10	23.743	4.051
	B	30.089	10	23.743	6.346
	C	32.928	0	0.0	32.928
C_{60}	A	42.153	0	0.0	42.153
	B	42.956	0	0.0	42.956
	C	43.272	2	4.749	38.523
	D	44.450	2	4.749	39.701
	E	45.163	2	4.749	40.414
	F	45.892	4	9.497	36.395
	G	46.150	4	9.497	36.653
	H	46.183	4	9.497	36.686
	I	46.719	4	9.497	37.222
	J	48.546	20	47.486	1.060

symmetry (structure B of Fig. 1) and can be viewed as the limiting case in which five windows have been opened in the fullerene structure. The open-window mechanism also helps to release the strain energy of the fullerene isomer of C_{32}. This fullerene lowers its energy in 0.42 eV by breaking four carbon-carbon bonds between adjacent pentagons giving rise to four open windows in the fullerene cage. The bowl structure (a portion of the C_{60} fullerene) is 6.59 eV higher in energy than the minimum energy structure.

It is well established that the minimum energy structure of C_{60} is the buckminsterfullerene, the fullerene with I_h symmetry (structure A of Fig. 2). However, one should keep in mind that there are 1812 topologically different fullerene isomers of C_{60} [4] which differ one from another only in the relative positions of the 12 pentagons and the 20 hexagons forming the fullerene cage. What makes the buckyball structure "special" is that it is the only 60-atom fullerene which satisfies the isolated pentagon rule, *i.e.*, there are no adjacent pentagons in the structure. In the buckyball every pentagon is completely surrounded by hexagons, which is what minimizes the local curvature and thus the strain energy of this structure. Stone and Wales [30] proposed a basic transformation for ring rearrangement in a fullerene cage which provides a mechanism for the stepwise conversion of most of the fullerene isomers of C_{60} into the most stable, buckyball, structure. The necessary last step before reaching the buckyball structure is isomer B of C_{60} (see Fig. 2) which is obtained from the buckyball by performing a single Stone-Wales transformation [31]. This isomer (having C_{2v} symmetry) contains two pairs of adjacent pentagons and is 0.8 eV higher in energy than the buckyball. (The LDA calculation performed by Yi and Bernholc [32] gives an energy difference of 1.6 eV.) The loss of stability of isomer B of C_{60} with respect to the buckyball can be related to the formation of two pairs of adjacent pentagons with the consequent local increase in the curvature and in the strain energy (see Tab. 1).

Besides the perfect fullerenes, we have found many fullerene-based isomers of C_{60} which are produced by opening one or several windows in a fullerene cage (a selection of those isomers is shown in Fig. 2). The strain energy released by opening one window in a fullerene cage does not compensate the formation of dangling bonds and thus the open-window isomers are higher in energy than the corresponding perfect fullerenes (see Fig. 2 and Tab. 1). The net cost of opening one window between two adjacent pentagons in isomer B of C_{60} is 0.316 eV whereas the cost of opening one window between a pentagon and a hexagon is much higher (2.207 eV in isomer B and 2.297 eV in the buckyball (isomer A)). This clearly shows that there is a local loss of stability in a fullerene cage due to the presence of adjacent pentagons. Isomers with two or more open windows are higher in energy than the one-window isomers. As the number of open windows increases, the fullerene structure becomes less apparent. These higher-lying isomers can be characterized as distorted cage structures containing large rings or as even more open structures intermediate between a tube and a deformed bowl (see structures K and L of Fig. 2). Graphene-like isomers, *e.g.*, J structure of Figure 2, are at least 6.2 eV above the minimum energy structure. The large number of dangling bonds present in these structures is responsible for their relatively high energy.

From the previous presentation it is apparent that the minimum energy structures as well as the isomer hierarchy of C_N clusters ($N \leq 60$) can be interpreted in terms of two simple concepts, *i.e.*, the strain energy of a curved surface, on one hand, and the number of dangling bonds in the cluster, on the other hand. Carbon clusters tend to form cage structures in order to minimize the number of dangling bonds. The price to pay is the strain energy associated with the curvature of the cluster surface. Clearly, the strain energy (per atom) is larger for smaller cluster sizes. The trade off between these two effects will determine the energy ordering of the different structures. Thus, small clusters prefer planar structures with no curvature although the relative number of dangling bonds is high (nine in the case of C_{13}). By the size of 20 atoms it is already favorable to curve a little the structure forming a bowl, reducing by two the number of dangling bonds with respect to the planar isomer. For C_{32} the fullerene isomer, with no dangling bonds, is lower in energy than the bowl structure which has ten dangling bonds. But the strain energy of this small fullerene is still quite high. Opening four windows in the cage creates eight dangling bonds. However, it also releases a large amount of strain energy which results in lowering the energy of the cage with windows. For C_{60} the fullerene isomers, with no dangling bonds, are more stable than more open structures, including the graphitic-like isomers. Among the C_{60} fullerenes, the buckyball is the lowest one since it minimizes the local curvature across the fullerene surface due to the absence of pairs of adjacent pentagons.

3.2 Thermal behaviour

To investigate the finite-temperature behaviour of small carbon clusters and fullerenes we have performed constant energy molecular dynamics simulations over a wide range of cluster energies corresponding to cluster temperatures ranging from $T = 0$ K up to $T \sim 5000$ K, when the thermal decomposition (fragmentation or evaporation) of the cluster occurs. By scanning over cluster energies we generate the equation of state of the cluster, also called the caloric curve, which gives the thermal response of the cluster to an increase in energy, *i.e.*, the cluster temperature as a function of its total energy. The cluster energy is stepwise increased by scaling up (with a scaling factor between 1.1 and 1.5) the velocities of all the atoms in the cluster between successive MD runs of 20 to 50 ps each. The starting point for the heating up process is a zero temperature configuration of the cluster corresponding to either the minimum energy structure or some selected isomer. Different isomers give rise to different branches of the caloric curve. For a given total energy of the cluster the dynamical temperature is defined in the usual way in dynamical simulations

$$k_{\mathrm{B}}T = \frac{2}{3n-6}\,\langle E_{\mathrm{kin}}\rangle_t\,, \tag{9}$$

i.e., the time average (represented by $\langle\ \rangle_t$), over the entire trajectory, of the instantaneous kinetic energy E_{kin} of the cluster per degree of freedom equals half of the thermal energy given by $k_{\mathrm{B}}T$. k_{B} is the Boltzman constant and n is the number of atoms in the cluster. Clearly this definition of cluster temperature implicitly assumes that the cluster remains as a single cohesive (unfragmented) entity along the whole trajectory.

Figure 3 shows the branches of the caloric curve of C_{20} generated from the bowl minimum energy structure (geometry A of Fig. 1), the fullerene isomer (geometry C), and a piece of diamond (geometry D), respectively, and the branches of the caloric curve of C_{60} generated from the buckyball minimum energy structure (geometry A of Fig. 2) and isomers B and D. The horizontal separation between branches at zero temperature corresponds to the energy difference between the corresponding isomers. The low-temperature behaviour of the clusters is quasi-harmonic (as expected from a classical treatment) and the cluster temperature increases linearly with increasing total energy at the rate given by the equipartition theorem. For comparison we have plotted in Figure 3 the "harmonic" caloric curves for $n = 20$ and 60. Clearly the clusters behave as solid-like at low temperatures. The atoms perform oscillations around their equilibrium positions without changing the overall shape of the cluster. As the temperature is increased the caloric curves start to deviate from the harmonic limit. This indicates that the contribution of the anharmonic part of the potential is already significant. Superimposed on this continuous and smooth change in slope we observe abrupt jumps in some branches of the caloric curves occurring at well defined values of the total energy. At still higher temperatures the caloric curves lose completely their smooth (apart from the well defined jumps) almost linear behaviour. All the branches of the caloric curve of a given cluster size tend to merge together in a single "noisy" curve. Notice that the caloric curves end up (*i.e.*, cluster fragmentation or evaporation occurs) before recovering an almost constant slope regime, common to all the branches, which would correspond to the liquid-like phase of the clusters.

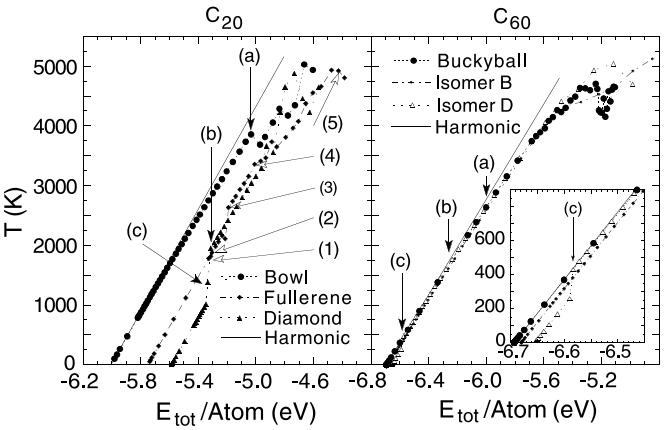

Fig. 3. Caloric curves of C_{20} and C_{60}. The branches of the caloric curve of C_{20} are generated from the bowl (minimum energy structure, isomer A of Fig. 1), the fullerene (structure C) and diamond-like (structure D) isomers. The full arrows indicate the first isomerization transition found in each isomer: (a) a window opens in the bowl structure, (b) a window opens in the fullerene isomer, and (c) the diamond-like isomer transforms into a tube-like structure. Arrows (1) to (5) refer to data presented in Figure 6. The branches of the caloric curve of C_{60} are generated from the buckyball (minimum energy structure, isomer A of Fig. 2) and isomers B and D. The full arrows indicate the first isomerization transition found in each isomer: (a) a window opens in the buckyball structure, (b) a window opens in isomer B, and (c) isomer D transforms into the buckyball. The harmonic limit is also shown as a solid line (see text for further explanation).

The changes in the slope of the caloric curves are clearly reflected in the specific heat. Instead of considering the "usual" definition of specific heat, *i.e.*, variation of energy with temperature per atom, we consider here the specific heat per degree of freedom given by

$$c_{\mathrm{v}} = \frac{1}{(3n-6)}\,\frac{\mathrm{d}E}{\mathrm{d}T}\,. \tag{10}$$

Figure 4 shows the specific heat per degree of freedom of the minimum energy structures of C_{13}, C_{20}, C_{32}, and C_{60}. At low temperatures and for all cluster sizes, c_{v} goes exactly to the classical (harmonic) limit, *i.e.*, $c_{\mathrm{v}} = k_{\mathrm{B}}$ [33].

The different features in the caloric curves can be correlated with structural changes of the clusters, *i.e.*, isomerization and phase transitions. However, from solely the caloric curves it is not possible to extract information on the type of structural transformations being experienced by the clusters as their temperature is increased. A measure and characterization of the movements of the atoms and of the associated structural changes in the cluster is

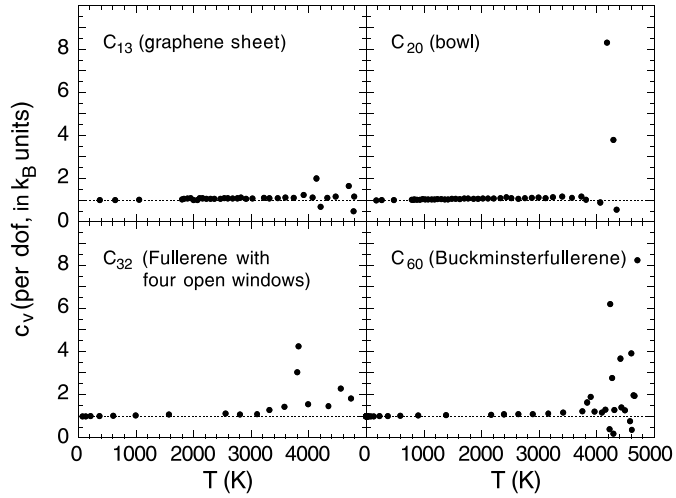

Fig. 4. Specific heat per degree of freedom (dof) as a function of cluster temperature of the minimum energy structures of C_{13}, C_{20}, C_{32}, and C_{60}. The dashed lines indicate the classical limit $c_{\rm v}(\text{per dof}) = k_{\rm B}$ (see text).

given by the relative root mean square bond length fluctuation δ

$$\delta = \frac{2}{n(n-1)} \sum_{i<j} \frac{\left(\langle r_{ij}^2\rangle_t - \langle r_{ij}\rangle_t^2\right)^{\frac{1}{2}}}{\langle r_{ij}\rangle_t}, \qquad (11)$$

where r_{ij} is the instantaneous distance between atoms i and j and the sum runs over all the pairs of atoms in the cluster. The interpretation of δ is based on the Lindemann criterion. Small ($< 10\%$) values of δ correspond to solid-like clusters with well defined structures, large ($> 20\%$) values of δ correspond to liquid-like clusters in which the atoms perform diffusive types of motions, and a sharp increase (over a finite-temperature range) of the magnitude of δ between those limiting values is the signature of the solid-to-liquid phase transition.

Figure 5 shows δ as a function of cluster energy for the same isomers of C_{20} and C_{60} considered in Figure 3. There is a correlation between the features in the caloric curves and the behaviour of the corresponding δ-curves. At low temperatures the value of δ is small ($< 10\%$) in agreement with a solid-like cluster. The discontinuities exhibited by several branches of the caloric curves, originating in isomers other than the minimum energy structure, at intermediate temperatures are reflected as small peaks or discontinuities in the corresponding δ-curves. The small value of δ in the peaks and discontinuities rule out their interpretation as a solid-to-liquid phase transition of the clusters. They arise from isomerization transitions which take the clusters from higher- to lower-energy regions of the configuration space with the corresponding increase in cluster temperature. Moreover the smooth behaviour of both the caloric and the δ-curves after the transition seems to indicate that the cluster keeps a solid-like character about a lower-energy isomer. At high temperatures the value of δ increases steeply, which correlates with the irregular behaviour of the caloric curves in this temperature

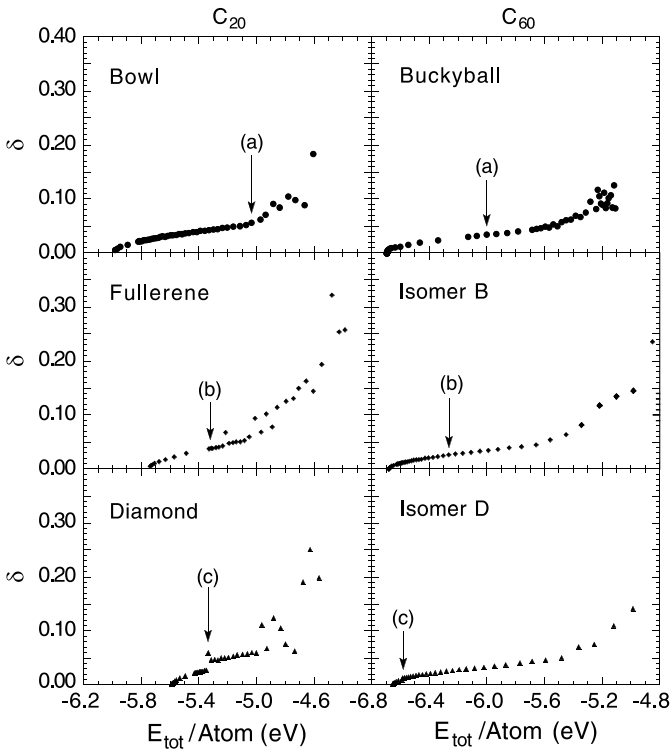

Fig. 5. Root mean square bond length fluctuation, δ, as a function of cluster energy for the same isomers of C_{20} and C_{60} considered in Figure 3. The full arrows have the same meaning as in that figure.

range. The sharp increase of δ is characteristic of the solid-to-liquid phase transition. However, there is not a high-temperature range characterized by a high value of δ, in clear correspondence with the lack of a high-temperature constant slope regime in the caloric curves. This reflects that "free" carbon clusters start to evaporate atoms or C_2 or C_3 units before fully developing a liquid-like phase. The lack of a fully developed liquid-like phase in small carbon clusters is in contrast with the presence of a well developed liquid-like phase in small "free" Lennard-Jones and metallic clusters. The phase diagram of bulk carbon shows that the liquid phase exists only under pressure. Similarly one can find a liquid-like phase in small carbon clusters by enclosing them in a box simulating the conditions of clusters under pressure.

Dynamical aspects of the finite-temperature behaviour of small carbon clusters can also be investigated. One can follow the structural changes of the clusters as a function of time by recording the time evolution of some dynamical magnitude sensitive to the cluster structure. One such magnitude is the short-time-averaged kinetic energy ($\langle E_{\rm kin}\rangle_{\rm sta}$). The time average is performed over a short period of time (typically 0.1 ps which is the time corresponding to a few characteristic vibrational periods of the cluster) to damp down the fluctuations in the kinetic energy due to the vibrational motions. Therefore, for a given total energy of the cluster, the value of $\langle E_{\rm kin}\rangle_{\rm sta}$ or, equivalently, the value of $\langle V\rangle_{\rm sta}$ (since the total energy is

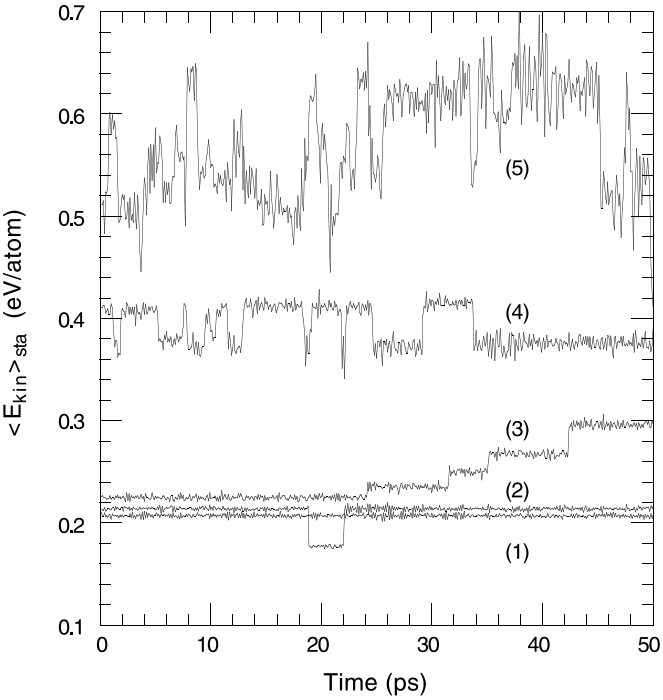

Fig. 6. Time-dependent short-time-averaged kinetic energy for several trajectories extracted from the branch of the caloric curve of C_{20} originating in the fullerene isomer. The trajectories ((1) to (5)) are indicated by an empty arrow on Figure 3. The total energies per atom (in eV) of these trajectories are: (1) −5.33, (2) −5.31, (3) −5.21, (4) −5.01, and (5) −4.43. (For the definition of the short time averages and the explanation of the jumps in the individual trajectories see text.)

constant, $\langle E_{\rm kin}\rangle_{\rm sta}$ and $\langle V\rangle_{\rm sta}$ are complementary quantities) characterizes each well of the potential energy surface, that is, each isomeric form of the cluster. Changes in the value of $\langle E_{\rm kin}\rangle_{\rm sta}$, besides small remnant fluctuations, correspond to structural transformations, *i.e.*, isomerization transitions. To clearly identify the structural transformations taking place as a function of cluster energy as well as the isomers involved in those transformations, we combine, for many trajectories along the different branches of the caloric curves of C_{20} and C_{60}, the study of the time dependence of $\langle E_{\rm kin}\rangle_{\rm sta}$ with a thermal quenching analysis (see Sect. 3.1 above) of those trajectories. As an illustration, Figure 6 shows the time dependence of the short-time-averaged kinetic energy for several trajectories (corresponding to different total energies of the cluster) selected from the branch of the caloric curve of C_{20} originating in the fullerene isomer. $\langle E_{\rm kin}\rangle_{\rm sta}$ is a piecewise constant function. The thermal quenching analysis confirms that the discontinuities in $\langle E_{\rm kin}\rangle_{\rm sta}$ arise from isomerization transitions in the cluster and that a single isomer defines the cluster dynamics within each finite-size time interval with a constant value of $\langle E_{\rm kin}\rangle_{\rm sta}$. At low energies (see trajectory (1) of Fig. 6) $\langle E_{\rm kin}\rangle_{\rm sta}$ presents only small fluctuations around a constant value which characterizes the isomer generating the corresponding branch of the caloric curve. For each isomer, the lower-energy trajectory in which a structural change of the cluster takes place has been indicated by a full arrow in the caloric curves (Fig. 3) and, correspondingly, in the δ-curves (Fig. 5). Notice that for a given cluster size the minimum energy structure is more "resistant" to structural changes than higher-lying isomers, *i.e.*, higher temperatures (or energies) are required for thermally exciting isomerization transitions in the former than in the latter isomers. This empirical rule may be relevant for understanding the formation mechanism of different cluster structures.

The thermal quenching analysis shows that the first isomerization transition experienced by the bowl and the fullerene isomers of C_{20} and the buckyball and isomer B of C_{60} are, all of them, driven by the open-window mechanism. These structural changes of the clusters are clearly seen in the time dependent $\langle E_{\rm kin}\rangle_{\rm sta}$ (see, *e.g.*, trajectory (2) of Fig. 6). Surprisingly, however, most of these isomerization transitions do not produce appreciable features neither in the caloric curves (Fig. 3) nor in the δ-curves (Fig. 5). The reason is two-fold: on one hand opening a window is a "local" structural change which does not involve diffusive-type motions of the atoms in the cluster and, consequently, the value of δ remains small. On the other hand, as is apparent from the $\langle E_{\rm kin}\rangle_{\rm sta}$ curves, the time spent by the cluster in the higher-energy (lower kinetic energy) open-window isomer is only a small fraction of the total time of the trajectory. The time averages over entire trajectories do not reflect, then, the distinct dynamics of the open-window isomer. The first isomerization transition experienced by isomer D of C_{60} is also driven by the open-window mechanism. This transition transforms isomer D into the buckyball minimum energy structure of C_{60}. Although this isomerization transition involves only a "local" structural change in the cluster it produces a noticeable effect (a sharp jump up) in the caloric curve (Fig. 3) and a small discontinuity in the δ-curve (Fig. 5) because once the transition takes place the cluster stays in the buckyball structure, *i.e.*, the transition is not reversible within the time scale of our simulation run. Therefore the energies lower than the isomerization-transition energy reflect the dynamics of the D isomer whereas higher energies reflect the dynamics of the buckyball structure. The increase in temperature at the energy of the isomerization transition reflects the difference between the depths of the potential wells of the two isomers, D and A, respectively. The first structural change of the diamond isomer of C_{20} involves the break up of many bonds giving rise to a tubular structure. Similarly to the case of the D isomer of C_{60}, this isomerization transition is not a reversible process and well defined features appear both in the caloric (Fig. 3) and in the δ-curves (Fig. 5) associated with this transformation. Another example of a relatively low-temperature nonreversible isomerization transition process is the stepwise transformation of the fullerene isomer of C_{20} into a cage structure with five open windows and D_{5h} symmetry (trajectory (3) of Fig. 6). The stair-like behaviour of $\langle E_{\rm kin}\rangle_{\rm sta}$ arises from successive open-window isomerization transitions. A window mechanism has been proposed for explaining the formation of

endohedral fullerenes [34,35]. Our simulations show that the structures with open windows are metastable states of the clusters with a finite lifetime that provides further support for that mechanism. All the isomers here considered (other than the minimum energy structures) present low-temperature isomerization transitions towards lower-energy isomers which means that all these higher-lying isomers are "directly" connected to lower-energy regions of the potential energy surface. This property of the topography of the potential energy surface of small carbon clusters and fullerenes will, certainly, play an important role in the annealing of the clusters. However, the existence of mechanisms (as the open-window mechanism presented here) driving low-temperature structural transformations of the clusters is not a specific feature of carbon clusters. For instance a floater-vacancy mechanism [36] has been described (in Lennard-Jones and metallic clusters) giving rise to the melting of the cluster surface at lower temperatures than the homogeneous melting of the cluster. It has also been shown that an atom-exchange mechanism is responsible for the premelting stage found in some small metal clusters [37].

At a relatively high energy the branch of the caloric curve of C_{60} originating in the buckyball jumps down and joins the branch of the caloric curve originating in isomer B. At this energy the open-window isomerization transitions are quite frequent. The abrupt change in the buckyball branch of the caloric curve is not produced, however, by these open-window isomerization transitions but by the Stone-Wales transformation. As we have mentioned in Section 3.1 the Stone-Wales transformation is a process for ring rearrangement in a fullerene cage and it has been proposed [30] as the basic process for annealing fullerene structures down to their corresponding ground states. This transformation, however, has been shown to have a quite high (6-7 eV) activation barrier [32] that could prevent it from being an efficient annealing mechanism for fullerenes. The thermal quenching analysis of the trajectory in which this transformation occurs reveals that the mechanism of the Stone-Wales process involves isomerization transitions through intermediate isomers which connect the buckyball structure of C_{60} with isomer B. A multi-step process, as the thermally excited mechanism found here for the Stone-Wales transformation, was completely unexpected on the grounds of the structural optimizations performed by other authors [32,38,39]. What is probably more noticeable about the multi-step mechanism proposed here is that the step-to-step isomerization transition barriers are substantially smaller (none of them exceeds 2.6 eV) than the one for the global process (5.58 eV). As a consequence the intermediate metastable isomers connecting two fullerene structures may play an important role in defining the kinetics of the annealing process without relying on an autocatalysis mechanism [38]. A detailed description of the multi-step mechanism of the Stone-Wales transformation of the buckyball and the intermediate isomers involved in it has been given elsewhere [40].

From $\langle E_{\rm kin}\rangle_{\rm sta}$ (see, *e.g.*, trajectories (4) and (5) of Fig. 6) it is also apparent that as the cluster energy is increased the isomerization transitions become more and more frequent and involve more and more isomers. However, only when the energy range corresponding to the solid-to-liquid phase transition is reached do these increasingly frequent isomerizations produce a sharp increase in the value of δ and the collapse of all the branches of the caloric curve of a given cluster size. The thermal quenching procedure reveals that, even at the elevated temperatures involved at the end of the transition region, there are some isomers that are thermally isolated from each other (at least within the time scale of our simulation runs), *i.e.*, there is not a thermally activated pathway of isomerization transitions connecting them. This behaviour is another manifestation of the lack of a fully developed liquid-like phase in small carbon clusters. As an empirical rule we find that bowl-type and graphitic-like structures do not close into cage- or fullerene-like structures even though the reverse processes have been observed in our simulations. As an illustration Figure 7 shows a few representative snapshots, extracted from the simulations, of the thermally excited transformation of the buckyball structure of C_{60} into an "almost perfect" graphene sheet.

As we have mentioned above, in our simulations cluster fragmentation or evaporation occurs before the carbon clusters have fully developed a liquid-like phase. However, several high-temperature phases of carbon clusters, including the liquid-like phase [16,18] and a pretzel and a linked chains phase [17], have been described by other authors. Those phases are similar to the state of the clusters we find by the end of the solid-to-liquid transition region and none of them is thermally stable, *i.e.*, cluster fragmentation will occur if one waits long enough. Therefore, in our view, it would be more adequate to talk about "the solid-to-liquid transition region" instead of about a "distinct cluster phase". The thermal decomposition (fragmentation) of the cluster defines the end of the transition region. The actual range and extent of the transition region depend both on the heating rate and the length of the simulation runs. One should bear in mind that only those processes (either isomerization transitions or cluster fragmentation) with a lifetime of the order of or smaller than the simulation time will be observed in a MD run. On the other hand, since the reaction rates (inverse of the lifetimes) increase with energy, the temperature at which a certain process is observed in a simulation is largely determined by the simulation time. The clear implication is that, since the time scale of any simulation is shorter (by several orders of magnitude) than the experimental time scale, the predicted [15] melting or fragmentation temperatures will be larger than the experimental ones.

The thermal stability and fragmentation kinetics of C_{60} molecules in the gas phase has been measured directly [12] in the temperature range of 1100–1970 K on the millisecond time scale. These experiments provide an activation energy for the fragmentation process of $E_0 = 4.0 \pm 0.3$ eV. On the other hand, experiments on the thermal decomposition of C_{60} in the solid state [13,14] yield

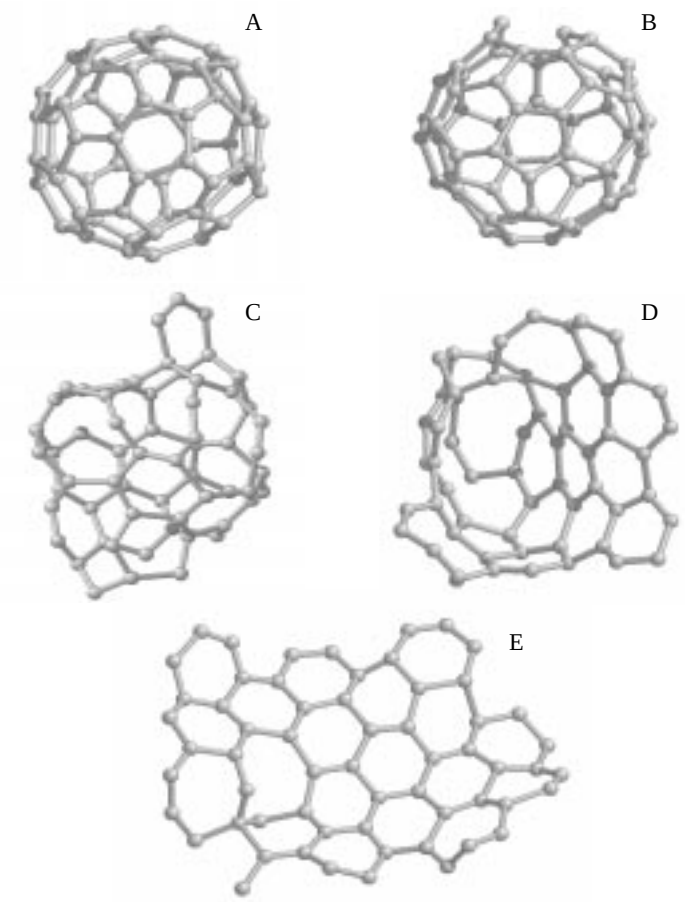

Fig. 7. Snapshots of the structural transformation of C_{60} from the buckyball minimum energy structure to a graphene-like structure. The frames have been extracted from the dynamical simulation runs at several temperatures: A: $T = 2500$ K, B: $T = 3800$ K, C: $T = 4200$ K, D: $T = 4600$ K, and E: $T = 4700$ K [23].

still lower activation energies (2.7 eV) for the unimolecular decay of the C_{60} molecule. These small values of the activation energy are inconsistent with the endothermicity (estimated in 10-13 eV [32,39]) of the dissociation reaction: $C_{60} \rightarrow C_{58} + C_2$, which is the primary fragmentation pathway of C_{60} [41]. As a tentative explanation it has been suggested [12,13] that the thermal fragmentation of C_{60} does not proceed directly from the buckyball minimum energy structure but rather it is a two-step process. The first step consisting of the structural transformation of C_{60}. Cluster fragmentation occurs, then, in a second step from a thermally excited isomeric form of C_{60}.

We can estimate the activation energy for fragmentation from a high-energy isomer. In the simulation originating in the buckyball, fragmentation of the molecule is observed at an excitation energy of 89 eV (this energy has been measured from isomer J of Fig. 2, since in this particular simulation C_{60} fragmented from a graphene-like isomer). The lifetime of the thermally excited C_{60} molecule (at this excitation energy) is of the order of the length of each individual simulation run (20 ps). Then, the rate constant (inverse of the lifetime) for fragmentation is $K = 0.05$ ps^{-1}. In the RRK (Rice-Ramsperger-Kassel) model (the simplest statistical approach to unimolecular processes [42]) the rate constant as a function of excitation energy E is given by

$$K(E) = \nu \left(\frac{E - E_0}{E} \right)^{s-1} , \qquad (12)$$

where E_0 is the activation energy, s is the number of vibrational degrees of freedom, and ν is a frequency proportionality factor. Taking $\nu = 800$ cm^{-1} which is a characteristic frequency for carbon, we obtain from equation (12) an activation energy of $E_0 = 3.1$ eV which is in fair agreement with the experimental results. Our simulations, then, provide full support to the two-step mechanism for the thermal decomposition of C_{60}. As we have shown, the thermal excitation of C_{60} produces profound structural changes in this molecule, and cluster fragmentation takes place from a high-energy configuration of the molecule. Moreover, the activation energy for this two-step fragmentation process comes out lower than (less than half) the one-step fragmentation energy for the minimum energy structure, in agreement with the experiments.

A quite different result is obtained, however, in laser-induced dissociation experiments [41]: C_2 units are ejected from fullerene cages preserving the cage structure of the carbon clusters. MD simulations of fullerene fragmentation [43] in which the excitation energy is suddenly delivered into the fullerene cage also produce ejection of C_2 directly from the fullerene cage. This one-step fragmentation mechanism is in contrast with the two-step thermal decomposition of fullerenes described above. In our view, the fragmentation mechanism actually followed by the clusters is largely determined by the rate at which the excitation energy is delivered into the cluster. At high excitation energies cluster reconstruction and cluster fragmentation are two competing processes. Slow heating rates of the clusters allow for cluster reconstruction prior to fragmentation (two-step process) whereas a fast increase in the cluster temperature will produce fragmentation (one-step process) before any structural transformation of the cluster takes place.

4 Conclusions

This paper has been devoted to the theoretical study of the thermal properties of small carbon clusters and fullerenes. We have performed constant energy Molecular Dynamics simulations over a wide range of temperatures ranging from $T = 0$ K to $T \sim 5000$ K. The interactions between the carbon atoms in the clusters are mimicked by the many-body semi-empirical Tersoff potential. This potential has proved reliable for describing the covalent bond in carbon systems. We have obtained about 50 to 100 different isomers for each cluster size by applying the thermal quenching procedure. The underlying rules determining the minimum energy structures as well as the isomer hierarchy of carbon clusters are, on the one hand, minimization of the strain energy (due to the curvature

of the cluster surface) which opposes the formation of cage structures and, on the other hand, minimization of the number of dangling bonds in the cluster which favors the cage isomers. The knowledge of the possible isomeric forms of the clusters helps in the interpretation of the phases and phase changes in the clusters. The thermal (*i.e.*, caloric curve, δ, and specific heat) and the dynamical (*i.e.*, time-dependent short-time-averaged kinetic energy) characteristics of carbon clusters and fullerenes have been analyzed as a function of temperature, not only for the minimum energy structures but also for some selected isomers. The low-temperature thermal behaviour of the clusters is fully characterized by the classical (harmonic) limit. Isomerization transitions are observed at temperatures lower than the ones corresponding to the melting-like transition region. Moreover, higher-lying isomers begin to experience structural transformations at lower temperatures than the corresponding minimum energy structures. These low-temperature isomerization transitions observed in higher-lying isomers drive the clusters from higher- to lower-energy regions of the potential energy surface and, consequently, they are not reversible within the time scale of our simulation runs. The topography of the potential energy surface (the higher-lying isomers are directly connected to lower-lying isomers) together with the possibility of low-temperature isomerization transitions may be key elements for understanding the annealing processes in clusters, for instance why the buckminsterfullerene is the only isomer of C_{60} which has been isolated in macroscopic quantities. We have also found that carbon clusters do not fully develop a liquid-like phase. However, cluster reconstruction plays an important role in the thermal decomposition of the clusters. Our simulations support the interpretation of the thermal decomposition of carbon clusters as a two-step process. First the structural transformation of the cluster takes place and then cluster fragmentation occurs from a high-energy configuration. Combining the simulation results with a simple statistical model for unimolecular processes we find an activation energy for the thermal decomposition of C_{60} in fair agreement with the experimental data. We cannot rule out other possible mechanisms (for instance decomposition in one step directly from the ground state) for the decomposition of carbon clusters. However, it seems that the fragmentation mechanism is determined by the nature of the excitation process. Thermal decomposition (slow heating rate) would proceed in two steps whereas laser-induced dissociation (sudden delivery of the excitation energy) would proceed in one step. This seems to indicate that the formation of different carbon structures could be favored by using different cooling rates. Clearly more work is needed for understanding and characterizing the growth mechanisms leading to the formation of different carbon-based structures.

Work supported by DGES (Grant PB95-0720-C02-01), Junta de Castilla y León (Grant VA72/96), Fundación Domingo Martínez, European Community TMR contract ERBFMRX-CT96-0067 (DG12-MIHT), and Centre de Computació y Comunicaciones de Catalunya. M.J.L. acknowledges a contract granted by MEC, program I+D, associated to the project PB95-0720-C02-01.

References

1. E.A. Rohlfing, D.H. Cox, A. Kaldor, J. Chem. Phys. **81**, 3322 (1984).
2. H.W. Kroto, J.R. Heath, S.C. O'Brien, R.F. Curl, R.E. Smalley, Nature **318**, 162 (1985).
3. W. Krätschmer, L.D. Lamb, K. Fostiropoulos, D.R. Huffman, Nature **347**, 354 (1990).
4. D.E. Manolopoulos, Chem. Phys. Lett. **192**, 330 (1992).
5. S. Iijima, Nature **354**, 56 (1991).
6. D. Ugarte, Nature **359**, 707 (1992).
7. A. Krishnan, E. Dujardin, M.M.J. Treacy, J. Hugdahl, S. Lynum, T.W. Ebbesen, Nature **388**, 451 (1997).
8. N.S. Goroff, Acc. Chem. Res. **29**, 77 (1996); and references therein.
9. D.M. Deaven, K.M. Ho, Phys. Rev. Lett. **75**, 288 (1995).
10. J.R. Chelikowsky, Phys. Rev. Lett. **67**, 2970 (1991); X. Jing, J.R. Chelikowsky, Phys. Rev. B **46**, 5028 (1992).
11. Y. Yamaguchi, S. Maruyama, Chem. Phys. Lett. **286**, 336 (1998); S. Maruyama, Y. Yamaguchi, Chem. Phys. Lett. **286**, 343 (1998).
12. E. Kolodney, B. Tsipinyuk, A. Budrevich, J. Chem. Phys. **100**, 8542 (1994).
13. S.D. Leifer, D.G. Goodwin, M.S. Anderson, J.R. Anderson, Phys. Rev. B **51**, 9973 (1995).
14. M.R. Stetzer, P.A. Heiney, J.E. Fischer, A.R. McGhie, Phys. Rev. B **55**, 127 (1997).
15. B.L. Zhang, C.Z. Wang, C.T. Chan, K.M. Ho, Phys. Rev. B **48**, 11381 (1993).
16. E. Kim, Y.H. Lee, J.Y. Lee, Phys. Rev. B **48**, 18230 (1993).
17. S.G. Kim, D. Tománek, Phys. Rev. Lett. **72**, 2418 (1994).
18. S. Serra, S. Sanguinetti, L. Colombo, J. Chem. Phys. **102**, 2151 (1995).
19. M.J. López, P.A. Marcos, A. Rubio, J.A. Alonso, Z. Phys. D **40**, 385 (1997).
20. L. Verlet, Phys. Rev. **159**, 98 (1967); W.C. Swope, H.C. Andersen, J. Chem. Phys. **76**, 637 (1982).
21. J. Tersoff, Phys. Rev. B **37**, 6991 (1988); Phys. Rev. Lett. **61**, 2879 (1988).
22. G.C. Abell, Phys. Rev. B **31**, 6184 (1985).
23. Tersoff potential gives a melting temperature for carbon of about 6000 K whereas the experimental value is about 4300 K.
24. J.P.K. Doye, D.J. Wales, J. Chem. Phys. **102**, 9659 (1995).
25. G.E. Scuseria, Science **271**, 942 (1996).
26. R.O. Jones, G. Seifert, Phys. Rev. Lett. **79**, 443 (1997).
27. P.R. Taylor, E. Bylaska, J.H. Weare, R. Kawai, Chem. Phys. Lett. **235**, 558 (1995).
28. J.C. Grossman, L. Mitas, K. Raghavachari, Phys. Rev. Lett. **75**, 3870 (1995).
29. J.P.K. Doye, D.J. Wales, R.S. Berry, J. Chem. Phys. **103**, 4234 (1995).
30. A.J. Stone, D.J. Wales, Chem. Phys. Lett. **128**, 501 (1986).
31. S.J. Austin, P.W. Fowler, D.E. Manolopoulos, F. Zerbetto, Chem. Phys. Lett. **235**, 146 (1995).
32. J.-Y. Yi, J. Bernholc, J. Chem. Phys. **96**, 8634 (1992).

33. Some authors (see, *e.g.*, refs. [16] and [17]) have presented classical simulations that, apparently, do not complain with the classical limit. No explanation of this behaviour, which is against any expectation, has been offered.
34. M. Saunders, R.J. Cross, H.A. Jiménez-Vázquez, R. Shimshi, A. Khong, Science **271**, 1693 (1996).
35. R.L. Murry, G.E. Scuseria, Science **263**, 791 (1994).
36. H.-P. Cheng, R.S. Berry, Phys. Rev. A **45**, 7969 (1992).
37. J. Jellinek, I. L. Garzón, Z. Phys. D **20**, 239 (1991); Z.B. Güvenç, J. Jellinek, A.F. Voter, in *Physics and Chemistry of Finite Systems: From Clusters to Crystals*, Vol. I, edited by P. Jena, S.N. Khanna and B.K. Rao (Kluwer Academic Publishers, Dordrecht, 1992) p. 411.
38. B.R. Eggen, M.I. Heggie, G. Jungnickel, C.D. Latham, R. Jones, P.R. Briddon, Science **272**, 87 (1996).
39. R.L. Murry, D.L. Strout, G.K. Odom, G.E. Scuseria, Nature **366**, 665 (1993).
40. P.A. Marcos, M.J. López, A. Rubio, J.A. Alonso, Chem. Phys. Lett. **273**, 367 (1997).
41. S.C. O'Brien, J.R. Heath, R.F. Curl, R.E. Smalley, J. Chem. Phys. **88**, 220 (1988).
42. For more precise statistical treatments see, *e.g.*, M.J. López, J. Jellinek, Phys. Rev. A **50**, 1415 (1994).
43. C. Xu, G.E. Scuseria, Phys. Rev. Lett. **72**, 669 (1994).